



Corrosion inhibition of mild steel in 1 M HCl solution by Artemisia Abrotanum essential oil as an eco-friendly inhibitor

Z. Bensouda¹, E. Ellassiri¹, M. Galai³, M. Sfaira¹, A. Farah², M. Ebn Touhami³

¹ Laboratoire d'Ingénieries des Matériaux, de Modélisation et d'Environnement. Université Sidi Mohamed Ben Abdellah USMBA, Faculté des Sciences BP 1796-30000 Fès-Atlas, Morocco.

² Laboratoire de Chimie Organique Appliquée. Université Sidi Mohamed Ben Abdellah USMBA, Faculté des Sciences et Techniques. Route Immouzer Fès, Morocco.

³ Laboratoire d'Ingénierie des Matériaux et Environnement : Modélisation et Application, Faculté des Sciences, Université Ibn Tofail, BP. 133-14000, Kénitra, Morocco.

Received 22 Jul 2017,
Revised 07 Oct 2017,
Accepted 14 Oct 2017

Keywords

- ✓ Corrosion inhibitor,
- ✓ Mild steel,
- ✓ GC-MS,
- ✓ Polarization,
- ✓ EIS,
- ✓ Adsorption isotherms.

bensouda@yahoo.com ;
Phone: +212654649017

Abstract

In this study, the corrosion inhibition properties of the Artemisia Abrotanum Essential Oil (AAEO) on mild steel surface in 1 M HCl solution has been investigated using Gas Chromatography-Mass Spectrometry (GC-MS), weight loss, Tafel polarization, Linear Polarization Resistance (LPR), Electrochemical Impedance Spectroscopy (EIS) and Scanning Electron Microscope (SEM) techniques. The effect of acid concentration and temperature on the corrosion behaviour of mild steel in 1 M HCl with addition of essential oil was also studied. The obtained results indicated that AAEO has a good inhibiting effect. The protection efficiency increases with increasing AAEO concentration reaches up to 83.9 %. However, the inhibition efficiency of essential oil slightly decreases with the rise of temperature. Tafel polarization examination indicated that AAEO acts as a mixed type inhibitor with predominance anodic action. The Nyquist impedance plots presented a depressed capacitive loop at high-frequency range followed by a well-defined inductive loop at low-frequency range. However, the Nyquist plots were analyzed by fitting the experimental data to an appropriate equivalent circuit. The adsorption of AAEO on mild steel surface obeyed to Langmuir isotherm model. SEM micrographs confirmed the existence of a protective adsorbed film on the mild steel surface.

1. Introduction

Currently, the investigation of mild steel corrosion mechanisms has become a principal academic and industrial subject, particularly in acidic solutions [1]. This is because of enlarged industrial applications of the acidic media. The principal fields of utilization are industrial acid descaling, acid pickling, cleaning of boilers and heat exchangers, the petrochemical processes, and so on. Operations which are usually accompanied by acid consumption and considerable dissolution of the mild steel. The hydrochloric acid solution is one of the most aggressive media and frequently used in industry [2]. Consequently, the rate of corrosion at which mild steel is ruined in HCl solution is very important, particularly when soluble corrosion products are formed, necessitating the usage of corrosion inhibitors to reduce the corrosion attack on the metal surface. A corrosion inhibitor is a chemical compound or combination of compounds that, when introducing in the appropriate concentration and forms in the environment, reduces corrosion [3]. Various of synthetic compounds used in industry has been referred as successful corrosion inhibitors which mainly contain multiple bonds in the molecule, long alkyl chains, aromatic rings and heteroatoms such as oxygen, sulfur, and nitrogen which they act by adsorption on the metallic surface [4–7]. Besides, the molecular weight of synthetic inhibitors, the project surface area and the number of heteroatoms performed an essential role in calculating their inhibition efficiency [8]. Although numerous synthetic compounds presented good anticorrosive action, the majority of them are considered poisonous to humans and the environment. [9]. However, as a result of ecological risks, expanding consciousness of health and their high cost, consideration is being drawn towards discovering novel, cheaper, highly efficient, environmentally friendly and non-poisonous inhibitors. In recent years, vegetal

inhibitors also called “eco-friendly or green inhibitors”, has revived more attention because they are ecologically and environmentally acceptable, renewable sources of materials, inexpensive, and readily available. Indeed, eco-friendly inhibitors can be used as purified substance [10–12], plant extract [13,14], and essential oil [15–17]. All of this green corrosion inhibitors have been considered to be efficient corrosion inhibitors for metals in acidic media.

The object of this study is devoted to investigating the inhibition effect of the Artemisia Abrotanum Essential Oil, denoted hereafter (AAEO), and not reported to our knowledge, on the mild steel corrosion inhibition in normal hydrochloric solution (1 M HCl). In this regard, the aerial parts of Artemisia Abrotanum collected from Tinghir (south of Morocco), was chosen for this investigation. The extraction of AAEO is realized by hydrodistillation utilizing a Clevenger-type apparatus. The chemical composition of AAEO has been established utilizing gas chromatography (GC) and gas chromatography-mass spectrometry techniques (GC-MS). The present work describes the detailed investigating of the inhibition effect of AAEO on the corrosion behavior of mild steel surface in the corrosive environment (1 M HCl) at 303 K utilizing weight loss, electrochemical as well as Scanning Electron Microscopy (SEM) techniques. The effect of temperature on the corrosion rate and the adsorption were also studied in detail.

2. Materials and methods

2.1. Material and specimens preparation

The mild steel was used as a study material with the following weight percentage chemical composition: (0.21% C, 0.01% Al, 0.09% P, 0.38% Si, 0.05% S, 0.05% Mn and rest Fe) are used. For gravimetric measurements, corrosion inhibition study was performed using coupons measuring with a rectangle form $3 \times 1 \times 0.05 \text{ cm}^3$ prepared from mild steel whereas coupons measuring of size $6 \times 1 \times 0.05 \text{ cm}^3$ with 1 cm^2 exposed surface were utilized as Working Electrode (WE) for electrochemical measurements. The mild steel specimens were grinding progressively with emerge paper SiC, from 60 to 2000 grade. Then, the samples were cleaned by washing with bidistilled water, defatted by absolute ethanol and dehydrated with acetone at 303 K before being immersed into the corrosive media so that all samples were in similar condition.

2.2. Inhibitor

The aerial parts dry of Artemisia Abrotanum were altogether washed with bidistilled water, split into small portions, then extracted utilizing a Clevenger-type apparatus as indicated in the European pharmacopeia[18]. AAEO yield was expressed in mL/ 100 g of dried vegetal material. The yield of the essential oil was approx. 1.16%.

About 2 μL of the essential oil with n-hexane was analyzed to Gas Chromatography - Mass Spectrometry (type QP2010 Shimadzu[®]) analysis by Trace gas chromatography /Polaris Q (Gas Chromatography - Mass Spectrometry, Thermo-Electron[®]). The column of gas chromatographic used the helium as mobile phase, it is a 95% dimethyl-polysiloxane and 5% phenyl with a length of 30 m, a layer thickness of 0.25 μm , and an interior diameter of 0.24 μm .

2.3. Medium

The corrosive solution, 1 M HCl was obtained by dilution of an analytical chemical reagent grade 37% HCl (Merck[®]) with doubly distilled water. The concentration ranges of AAEO used was 0.5 to 2 g L^{-1} .

2.4. Gravimetric method

The gravimetric experiments were realized in a double-walled glass cell containing 50 mL of the corrosive solution with and without diverse concentrations of essential oil. The double-walled glass cell was conserved in an air thermostat maintained at 303 K. The apparent surface area of coupons used was of 6.4 cm^2 and the immersion time was 6 h. The gravimetric results of each coupon were determined before and after experiments in the inhibited and uninhibited medium using an analytical balance (exactness 10^{-3} g). Every value is the means of triplicate tests. The inhibition efficiency ($\eta_{WL}\%$) for the gravimetric method is studied using corrosion rates (W_{corr}) according to following Equation 1:

$$\eta_{WL} \% = \left(\frac{W_0 - W_{inh}}{W_0} \right) \times 100 \quad (1)$$

where W_0 and W_{inh} are the corrosion rates of a sample in the absence and presence of AAEO.

2.5. Morphological investigation

Morphology of metal surface after its exposure to the corrosive solution (1 M HCl) with and without 2 g L⁻¹ of AAEO for 24 h was observed by Scanning Electron Microscopy (SEM) technique. The SEM micrographs were taken using a FEI Quanta[®] 200 instrument.

2.6. Electrochemical techniques

Electrochemical Impedance Spectroscopy (EIS) measurements and the Potentiodynamic Polarization (PP) study, were utilized using a Bio-Logic[®] potentiostat piloted by EC-Lab[®] software. All electrochemical tests were realized in a conventional three electrodes electrochemical cell at 303 K with a coupon of metal utilized as WE, a Saturated Calomel Electrode (SCE) was used as the reference electrode and a platinum electrode as the auxiliary electrode. Moreover, WE is the same nature as their used for gravimetric measurements. However, WE was vertically immersed in the study solution and after starting an Open Circuit Potential (OCP) for a period of 0.5 hours to achieve stable corrosion potential (E_{corr}) value., the electrochemical measurements were performed.

PP curves were carried out from -900 mV_{SCE} to -100 mV_{SCE} with respect to E_{corr} at a scan rate of 1 mV/s. The calculated anodic Tafel lines (β_a) and the linear Tafel segments of the experimental cathodic curves (β_c) were extrapolated to the point of intersection to obtain E_{corr} and corrosion current density (i_{corr}) [10]. The inhibiting efficiency (η_{Tafel}) value for the Tafel method is calculated as according to Equation 2:

$$\eta_{Tafel} \% = \left(1 - \frac{i_{corr/inh}}{i_{corr}} \right) \times 100 \quad (2)$$

where i_{corr} represent the corrosion current density values without AAEO and $i_{corr/inh}$ is the corrosion current density values with AAEO.

$i_{corr/inh}$ and i_{corr} have been determined by only the cathodic polarization curve β_c at points 200 mV more negative than E_{corr} [19].

The Linear Polarization Resistance (LPR) was done by recording WE in different inhibitor concentrations from -15 to +15 mV_{SCE} around corrosion potential (open circuit potential) by 1 mV/min scan rate. The R_p values can be measured by calculating the slope of the linear part of current-potential plots (Stern & Geary) [20] according to the following Equation 3:

$$R_p = S \times \left(\frac{dE}{di} \right)_{i \rightarrow 0} \quad (3)$$

where dE is the difference in applied potential, S is the surface area of mild steel, and di is the difference in the current density. However, the protection efficiency ($\eta_{S\&G} \%$) for LPR technique is calculated by R_p using the relationship 4:

$$\eta_{S\&G} \% = \left(1 - \frac{R_p}{R_{p/inh}} \right) \times 100 \quad (4)$$

where $R_{p/inh}$ is the polarisation resistance values in the presence of essential oil, and R_p is the polarisation resistance values in the absence of essential oil.

EIS measurements were realized utilizing a transfer function analyzer (Bio-Logic[®] potentiostat), by a minor amplitude ac. signal of 10 mV rms, over a frequency spectrum from 100,000 Hz to 0.01 Hz at 303 K on air atmosphere with ten points per decade. However, a laptop controlled the measurements conducted at rest potentials after 0.5 h of immersion at E_{corr} . The impedance plots were given in the Bode and Nyquist representations. Furthermore, EIS data were analyzed and fitted with ZView[®] 2.80 software.

3. Results and discussion

3.1. Essential oil composition

In the present study, 30 volatile organic components from AAEO were identified through GC-MS analysis (Figure.1).

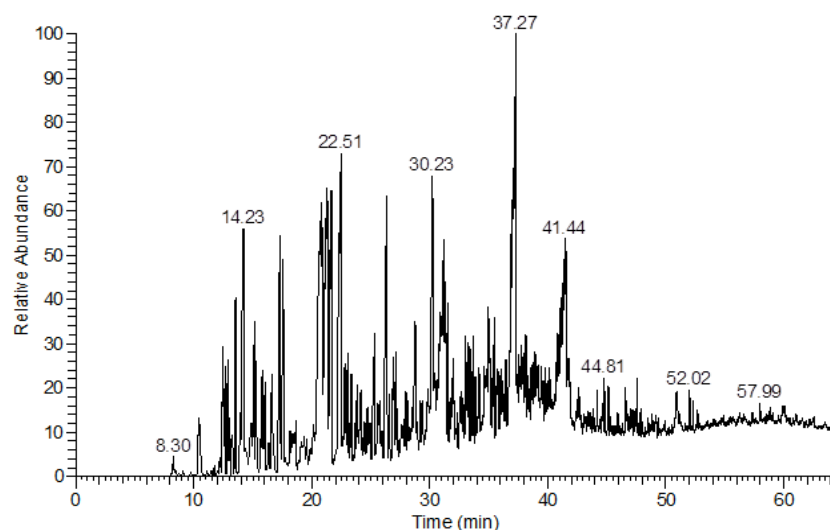


Figure1: Gas chromatography and gas chromatography - mass spectrometry AAEO spectre.

Characteristics of the identified components such as their chemical name and percentage among the total compounds of AAEO are presented in Table 1.

Table 1:Composition of AAEO.

Constituent	%	Constituent	%
Chrysanthenone	28.10	Thujyl neo-3-acetate	0.57
Camphor	26.67	Trans myrtanol	0.56
α -thujone	9.26	α -terpin-7-al	0.46
α -pinene	6.07	α -thujene	0.45
β -thujone	5.60	α -acetateterpinyl	0.42
β -elemene	3.86	Trans piperitol	0.40
Trans- β -terpineol	3.17	D-germacrene-4-ol	0.37
Germacrene	3.15	Myrcene	0.31
Trans- β -dihydroterpineol	1.80	α -terpinene	0.25
α -munrolene	1.41	α -caryophyllene	0.25
Terpin-4-ol	1.39	α -terpineol	0.24
Limonene	1.17	γ -terpinene	0.21
Davanone	1.13	Camphene	0.16
β -pinene	1.09	Cis- β -dihydroterpineol	0.15
Neo-iso-acetate isopulegol	0.61	Tricyclene	0.14

It is clear from Table 1 that among the total compounds, *Chrysanthenone* was the major compound identified in the essential oil (28.10%). Figure.2 presented the chemical structures of the major abundant compounds containing in the essential oil.

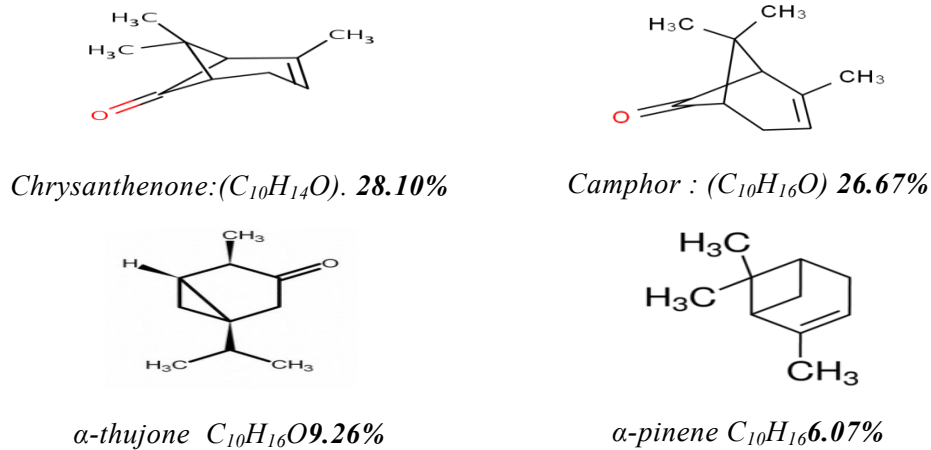


Figure 2: Chemical structures of the major compounds of AAEO.

3.2. Gravimetric and SEM study

The gravimetric monitoring by W_{corr} and η_{WL} is advantageous because of the simplicity of the method and it does not require very expensive equipment. Indeed, the weight loss experiments have been utilized by many researchers [5,10]. The values of W_{corr} and η_{WL} have been given by the gravimetric method using Equation 1 at diverse concentrations of AAEO and after six hours of immersion in corrosive solution (1M HCl) at 303 K are shown in Figure 3.

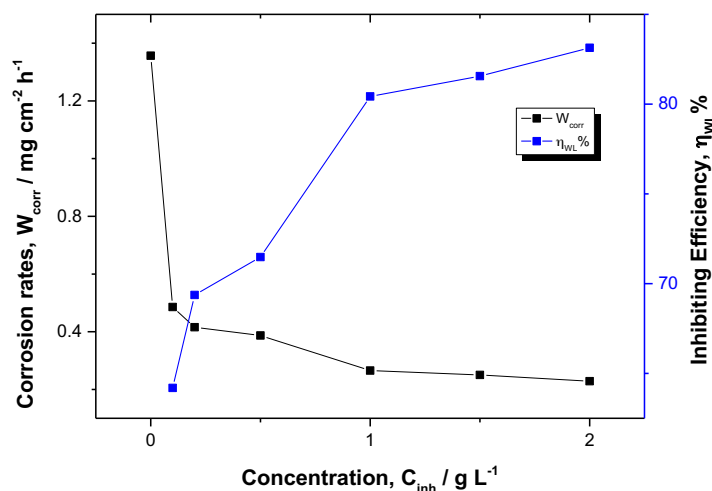


Figure 3: Relationship between corrosion rate W_{corr} and inhibiting efficiency η_{WL} of electrode exposed for 6 h in 1 M HCl at different concentrations of AAEO and at 303 K.

It is evident from Figure 3 that, W_{corr} decreases sharply with the rise in AAEO concentration, whereas the values of η_{WL} ameliorating with increasing AAEO and the maximum value reaches 83.14%. These results designate that AAEO may successfully protect metal from dissolving in the aggressive media and the essential oil is an effective corrosion inhibitor for mild steel in 1 M HCl solution. However, the productivity effect of essential oil may be ascribed to the adsorption of essential oil compounds at the metal surface [21]. Elements as Oxygen with a free pair of electrons as well as the π -electrons in the major compounds of AAEO (Figure 2) might support electron contribution to the vacant d-orbital of iron atoms, and so, the adsorption of the essential oil is favoured [22]. Moreover, the existence of the protonated elements, for example, oxygen can receive the electron from iron atoms [19]. The adsorption of the essential oil compounds on the liberated sites or new sites produced by corrosion kinetics of metal results in the creation of the protective film on the metal surface, which isolates metal surface from the aggressive solution [23]. Additionally, a covering phenomenon might likewise occur between AAEO molecules and corrosion products, which can obstruct the diffusion processes of the corrosive substances to the surface of mild steel [24]. However, it is difficult to identify a particular component of AAEO responsible for the observed inhibition of the inhibitor but the adsorption can do a synergistic effect of all molecules. The combined effect of all the compounds of AAEO contributes to this effective protection of the

corrosion of metal surface in aggressive solution(1M HCl)[25].The high-resolution SEM images (50 μm) of a metal surface in 1 M HCl solution with and without 2 g L^{-1} of AAEO after 24 h of immersion are given in Figure. 4.

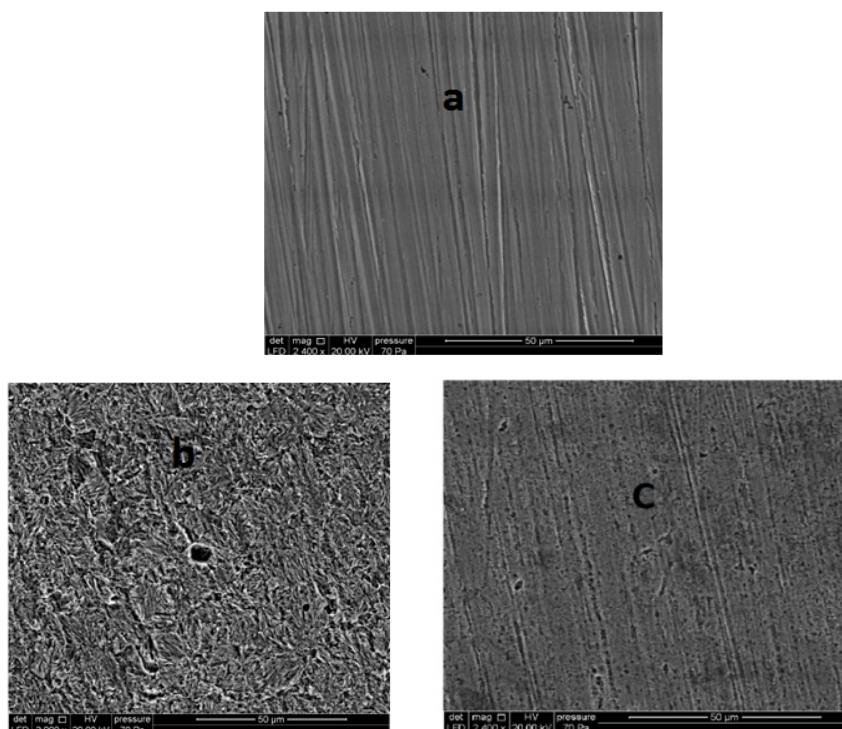


Figure 4:SEM images of the electrode surface: (a) electrode surface non - treated (after being polished only), (b) electrode surface for 24 h immersion in 1 M HCl and (c) electrode surface for 24 h immersion in 1 M HCl + 2 g L^{-1} of AAEO.

The surface morphology given in Figure.4a showed the SEM micrograph for the non-treated specimen of the metal surface. This result is recorded hither for the comparison with those of corroded specimen. Moreover, we have observed mechanical damage probably produced by abrading scratches on the electrode surface. Indeed, as it has appeared in Figure. 4b, the metal surface is extremely damaged, due to the electrode dissolution in 1 M HCl. Therefore, the surface of the metal is greatly porous. However, the morphology of metal surface is considerably changed when addition essential oil to the aggressive medium[26]. As shown in Figure. 4 c the dissolution rate of metal surface significantly reduced, a relatively smoother and less corroded attack show up by the presence of a protective film on the electrode surface[27]. The best protection is seen in the presence 2 g L^{-1} of AAEO (Figure. 4c) compared to that observed in Figure. 4b. So that, the electrode surface is protected counter the attack of the aggressive environment by this adsorption film and W_{corr} is considerably reduced, in the presence of AAEO. However, these results could support higher inhibition efficiency of AAEO [28].

3.3. Potentiodynamic polarization study

PP measurements have been utilized in order to obtain more information about the kinetics of the anodic and cathodic reactions. The influence of essential oil concentration on the anodic and cathodic polarization behaviour of working electrode in a normal hydrochloric solution containing various amounts of corrosion inhibitor has been investigated by PP measurements and the registered Tafel plots are given in Figure. 5. As a matter of fact, the anodic curves represent the iron dissolution reaction whereas the cathodic curves represent the hydrogen evolution reaction[29]. As can be seen from Figure.5, the addition of AAEO reduces the cathodic and anodic current density in the concentration area from 0.5 to 2 g L^{-1} and consequently hinders the acid attack of electrode in the aggressive medium[30]. The reduction in i_{corr} , and related W_{corr} pronounces more and more with the increasing AAEO concentration [31]. However, E_{corr} of mild steel nearly remains constant at the concentration range studied, there is a slight shift towards more positive potentials at higher concentrations with respect to the corrosion potential detected in the blank.

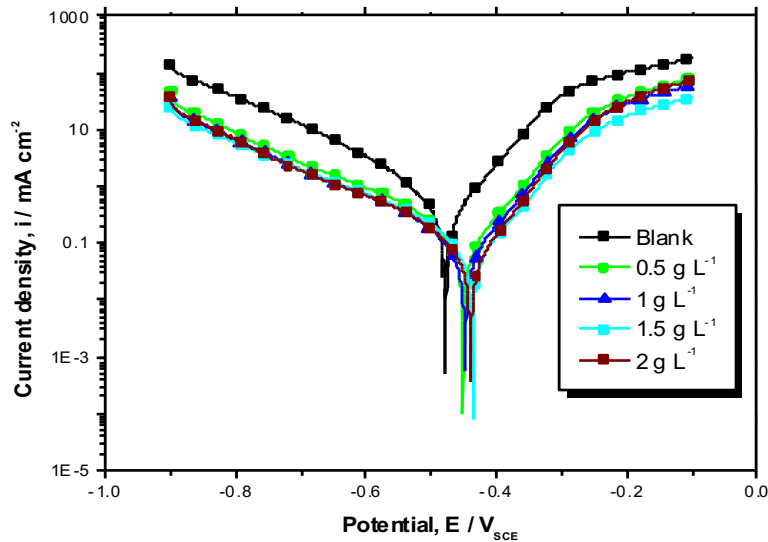


Figure 5: PP curves of mild steel in the corrosive solution (1M HCl) containing various concentrations of AAEO.

On the one hand, the cathodic Tafel curves offering rise to parallel lines designate that the introduction of essential oil to the corrosive medium doesn't change the mechanism of the hydrogen evolution reaction and the reduction of H^+ ions at the metal sites takes place principally by a charge transfer mechanism [32]. On the other hand, the anodic polarization curves don't display a considerable Tafel curve, maybe because of the existence of the impurities or corrosion products to form a non-passive film on the electrode surface. The presence of such impurities and the deposition of corrosion products don't result in a well-defined experimental anodic Tafel curves [33]. Therefore, the cathodic polarization curves are favored, versus to the anodic ones for obtaining i_{corr} utilizing the Tafel extrapolation method. It can be remarked from Figure 5 that the forms of the PP curves in presence of inhibitor are not considerably different from this in absence of inhibitor. The presence of AAEO decrease W_{corr} but doesn't modify other aspects of the behavior. This implies that AAEO doesn't modify the electrochemical reactions responsible for corrosion. Based on the positive shift in E_{corr} and the decrease of the cathodic and anodic current density after addition AAEO in aggressive medium, we can conclude that the inhibitor compounds can be considered as a mixed type inhibitor with predominance anodic action [33].

Table 2: Electrochemical data evaluated from Tafel and LPR methods for metal in 1 M HCl with and without AAEO at 303 K.

AAEO concentration / $g L^{-1}$	Tafel data			LPR data		
	E_{corr} mV/SCE	i_{corr} $\mu A cm^2$	$-\beta_c$ $mV dec^{-1}$	η_{Tafel} %	R_p $\Omega.cm^2$	$\eta_{S\&G}$ %
Blank	-479.51	623.73	168.5	-	59.4	-
0.5	-451.12	182.38	210.5	70.75	226	73.71
1	-448.08	126.47	207.1	79.72	307	80.65
1.5	-436.95	122.17	211.6	80.41	311	80.90
2	-439.67	111.68	206.2	82.09	344	82.73

As seen from Table 2 E_{corr} was displaced to less positive potential while i_{corr} was displaced to the lower current density region. It has been reported in the literature that inhibitor can be classified as an anodic or cathodic type when the displacement in E_{corr} is superior to $85 mV_{SCE}$ with reference to the uninhibited solution, otherwise inhibitor is considered as a mixed type. From Table 2 maximum displacement in E_{corr} value was around $43 mV_{SCE}$ and the cathodic Tafel slopes β_c values show a slight change with the addition of AAEO. The small variation of β_c , and the parallel cathodic Tafel lines are shown in Figure 5 suggest that the hydrogen evolution

reaction is underactivation control. These results indicate that essential oil acts as corrosion inhibitor by retarding the cathodic and anodic reactions and blocking the active sites by getting adsorbed on the metal surface [34]. That way, the surface area of mild steel accessible for H^+ ions are reduced while the actual reaction mechanism stays unaffected [9]. For that reason, the addition of essential oil reduces the anodic dissolution and also retards the cathodic hydrogen evolution reaction, designating that AAEO exhibit anodic and cathodic inhibition effects [35]. Consequently, AAEO can be classified as mixed type inhibitor with anodic predominance effect [36]. Besides, η_{Tafel} values increased with increase in AAEO concentration reaches to 82.09% at only 2 g L^{-1} and it is in agreement with η_{WL} given by gravimetric measurements.

The LPR experiments were used to ignore the effect of the electrode surface changes which can happen during PP at higher over-potentials in the potentiodynamic study [37]. The inhibition efficiency $\eta_{S\&G}$ % of AAEO on the electrode in the aggressive medium (1M HCl) was also studied using LPR technique. It is clear from Table 2, which R_p considerably increases with the rising in AAEO concentration, reaches to $344\ \Omega\ \text{cm}^2$ in presence of 2 g L^{-1} of inhibitor, while it is only $59.4\ \Omega\ \text{cm}^2$ for the blank solution. Besides, the increase in R_p values, suggests the development of adsorption phenomenon of AAEO compounds on the metal surface and blocking the surface against the corrosive attack more efficiently [38]. Moreover, the agreement between $\eta_{S\&G}$ and η_{Tafel} are pretty good.

3.4. EIS study

For obtained more information concerning the kinetics of mild steel processes and simultaneously the surface properties of the studied systems, EIS measurements were used. Figure. 6 shows the obtained Nyquist and Bode diagrams of metal in aggressive solution (1 M HCl) in the presence and absence of various concentrations of essential oil.

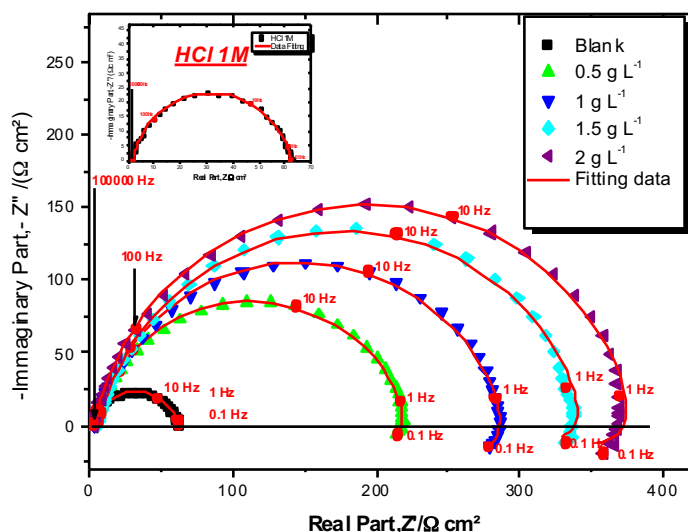


Figure 6: Complex plane impedance diagrams (Nyquist) of a mild steel in 1 M HCl containing different concentrations of AAEO.

It is clearly apparent in Figure.6 that EIS response of metal electrode in corrosive solution was considerably modified after the addition of AAEO concentrations. Moreover, the EIS spectra in presence of inhibitor increase with an increase in AAEO concentration, which indicates the amelioration in protection effect on metal corrosion surface. Indeed, the EIS spectra in the Nyquist diagrams illustration one depressed capacitive loop at high frequency (HF) range and one small inductive loop at low frequency (LF) range. The same behavior is shown in the literature [30,39]. At this point, the depressed capacitive loop was associated to charge transfer resistance in corrosion process and time constant of the electric double film [40]. So that, the depressed form of the capacitive loop reflects the surface inhomogeneity of interfacial origin. On the other hand, the small inductive R_2 -L loop can be related to the relaxation of adsorbed species like H^+_{ads} and Cl^-_{ads} on mild steel surface [35]. Indeed, it perhaps associated to the redissolution of the passivated surface at LF. Furthermore, for EIS spectra two equivalent circuits models were utilized to fitting the experimental results (Figure. 7). In this equivalent circuits model R_s is the solution resistance, CPE is the constant phase element, R_i is the polarization

resistance, $R_{ct} = R_1 + R_2$ corresponds to the charge transfer resistance. Besides, resistance R_2 and inductivity L might be associated with a slow LF process. Best fitting of experimental results is obtained utilizing the equivalent circuits models given in Figure 7[41]. Moreover, CPE utilized to elucidate the depression of the capacitance semicircle, which corresponds to surface inhomogeneity resulting from electrode surface roughness, dislocations, impurities formation of a porous film, adsorption of inhibitors[35].

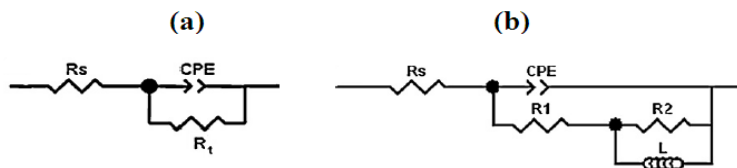


Figure 7: The equivalent circuits utilized for the fitted EIS spectra.

For characterization of depressed semicircles, a CPE was utilized according to the following Equation 5:

$$Z_{CPE} = Q^{-n} \times (j \times \omega)^{-n} \quad (5)$$

where Q is proportionality coefficient of CPE ($\mu F s^{n-1}$), j is an imaginary number with $j^2 = -1$, ω is the angular frequency in $rad s^{-1}$. $\omega_{max} = 2 \times \pi \times f_{max}$, where f_{max} is the frequency at which the imaginary part of the impedance is maximal ($-Z''_{im,max}$) and n represents the deviation from the perfect behavior ($0 \leq n \leq 1$).

The double layer capacitance (C_{dl}) can be mathematically calculated utilizing the Equation 6 [40]:

$$C_{dl} = \frac{Q \times \omega^{n-1}}{\sin\left(n \times \frac{\pi}{2}\right)} \quad (6)$$

The relaxation time constant (τ) can be calculated according the following Equation 7:

$$\tau = C_{dl} \times R_{ct} \quad (7)$$

The EIS parameters and the quality of fitting χ^2 , are presented in Table 3.

Examination of data archived in Table 3 indicates that in the whole concentration range, R_{ct} increase with AAEO concentration. This effect is correlated with the simultaneous diminution of C_{dl} . Moreover, the value of Q differs in a regular manner with AAEO concentration. However, the differences in Q and R_{ct} may be associated to the gradual displacement of H_2O molecules by essential oil compounds on the mild steel surface, that's why conduct to reduction in the number of active sites essential for the corrosion reaction[42].

Table 3: EIS parameters of electrode in corrosive solution (1 M HCl) containing different concentrations of AAEO at 303 K.

C_{inh}	R_s	R_1	R_2	R_{ct}	C_{dl}	τ	$10^4 Q$	n	L	ϕ	α	χ^2	η_{EIS}
$g L^{-1}$	Ωcm^2	Ωcm^2	Ωcm^2	Ωcm^2	$\mu F cm^{-2}$	ms	$\mu F s^{n-1}$		$H cm^{-2}$				%
Blank	1.42	61.15	-	-	113.1	0.0069	2.673	0.827	-	-0.622	58.12	0.0017	-
0.5	2.37	201.3	19.06	61.15	46.63	0.0102	0.971	0.840	21.62	-0.692	62.90	0.0058	72.24
1	3.15	246.4	41.5	220.3	34.50	0.0100	0.692	0.844	38.31	-0.693	63.24	0.0031	78.75
1.5	5.16	314.4	28.43	287.9	34.17	0.0116	0.690	0.845	57.29	-0.704	61.92	0.0011	82.16
2	2.64	342.4	38.01	342.8	26.49	0.0100	0.514	0.859	86.23	-0.731	67.42	0.0021	83.92

Moreover, the increase of n value after addition AAEO in aggressive solution (0.840-0.859) when compared to that achieved in the blank (0.827) can be explicated by some reduction of the initial surface inhomogeneity. However, the value of τ observed in the blank equal to 0.0069 s. After addition of inhibitor in 1M HCl results in an increase in τ value ($\tau = 0.0116$ s) which remains approximately unchanging. After increasing of essential oil, τ becomes considerably higher which means slow adsorption process. Besides, the obtained χ^2 values (0.0017-0.0058) in Table 3 indicates a good fitting to the proposed circuits models.

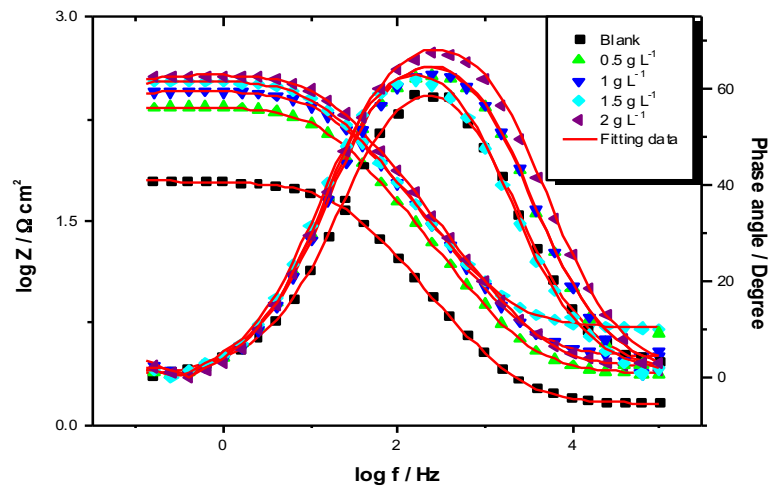


Figure 8: Bode plots for electrode in aggressive solution (1M HCl) containing various concentrations of AAEO at 303 K.

Figure.8 exemplified the corresponding the Bode impedance magnitude and the phase angle plots. It is clear from the phase angle plots that the single narrow peaks designate a single τ for the corrosion process at the mild steel/solution interface in both cases. The increase in the peak altitudes corresponds to an additional capacitive response to the mild steel/solution interface because of the presence of essential oil compounds at the interface [10]. On the one hand, the EIS at HF limits ($f = 10^4$ Hz) associated to the ohmic resistance of the adsorbed film and R_s . Moreover, at HF the phase angle (α) decrease quickly to 0° and the Bode impedance magnitude ($\log |Z|$) values tend to come near to zero. Its correspond to solution resistance. On the other hand, at a middle frequency, a linear relation between $\log |Z|$ against $\log f$ with a slope of Bode impedance magnitude plots (ϕ) close to -1 and α approaching to -62° can be remarked (Table 3). A true capacitive behavior is rarely obtained ($\alpha = 90^\circ$ and $\phi = -1$). It is apparent from Figure.8 at a middle frequency, that ϕ diverge from -1 and the maximum of α diverge from 90° . These different results are related to the deviation from the true capacitive behavior. Moreover, it can be associated with the rising of the standard rate constant of the protective film dissolution [43,44]. Similarly, the regular approach of α and ϕ to the true capacitive values after the addition of essential oil may be associated with decreasing the rate of a dissolution of mild steel.

The inhibition efficiency $\eta_{EIS} \%$ was determined by Equation 8:

$$\eta_{EIS} \% = \left(\frac{R_{ct/inh} - R_{ct}}{R_{ct/inh}} \right) \times 100 \quad (8)$$

where R_{ct} is the charge-transfer resistance values for 1M HCl and $R_{ct/inh}$ is the charge-transfer resistance values with different concentration of AAEO. The values of $\eta_{EIS} \%$ increase with increasing concentration of essential oil arrive at 83.92% when essential oil concentration reaches 2 g L^{-1} .

3.5. Comparison of the overall results

Comparison of the protection efficiency $\eta \%$ values for the examined concentration of AAEO achieved by four various techniques, namely gravimetric, PP curves (Tafel and Stern & Geary extrapolation) and EIS techniques for the metal in aggressive solution (1M HCl) were realized. Figure.9 shows a histogram of all results which can identify the gaps when comparing the obtained $\eta \%$ values.

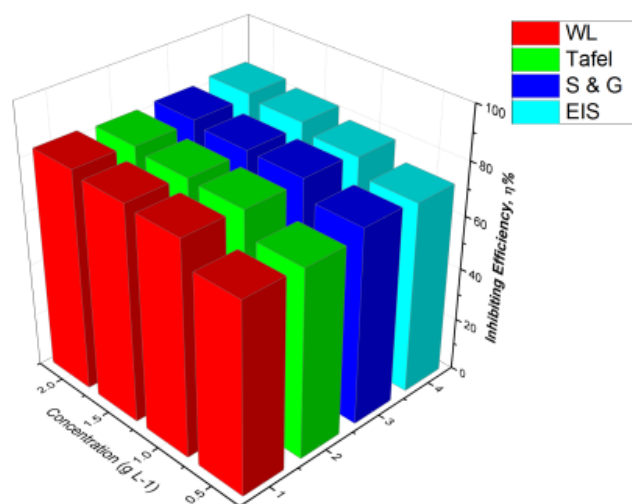


Figure 9: Comparison of η % for 1 M HCl solution with various concentrations of essential oil achieved by four various techniques at 303 K.

It is obvious from Figure.9 that the protection efficiency η %, determined from all methods illustrates a similar tendency and η % is high at all concentrations study of essential oil. The greatest η % was detected in the case of 2 g L^{-1} of AAEO concentration (cca 100%).

3.6. Effect of temperature

It is clear that the temperature can change the interaction between the acid medium and the mild steel surface. Moreover, the effect of temperature on the protection efficiency of AAEO was also investigated by gravimetric experiments in the temperature ranges 303–353 K in aggressive solution (1 M HCl) at 2 hours of immersion time with and without essential oil.

Table 4: Weight- loss data of the metal corrosion in absence and presence of 2 g L^{-1} of essential oil study at various temperatures after 2 h of immersion period.

Temperature / K	Corrosion rate $W_{corr} / \text{mg h}^{-1} \text{cm}^{-2}$		$E_{WL} \%$
	Blank	AAEO	
303	1.3567	0.2287	83.14
313	2.3217	0.4435	80.89
323	4.8517	1.1576	76.14
333	9.9035	2.6357	73.38
343	13.8185	4.0764	70.50
353	26.3414	8.4345	67.98

Inspection of results presented in Table 4 reveals that W_{corr} rise with rising temperature in absence and presence of essential oil. We likewise noted that $E_{WL} \%$ depends on the temperature. The diminution of $E_{WL} \%$ with the increase of temperature from 303 to 353 K, can be interpreted in term of physisorption character of essential oil compounds on the mild steel surface. However, it is obvious that the gravimetric is circa 19 and 36 times greater, at 353 K when compared to 303 K, in the blank and protective media, respectively. Though, it is necessary to note that the presence of essential oil slows down the average W_{corr} at all the investigated temperatures, by 4 times by comparison to the blank solution. Moreover, $E_{WL} \%$ seems little sensitive to the effect of temperature.

For the calculating the activation parameters including E_a , ΔS^* and ΔH^* for the corrosion reaction, the Arrhenius equation and its alternative Equation named the transition state equation was employed according to the following Equations 9 and 10:

$$W_{corr} = P e^{\frac{-E_a}{RT}} \quad (9)$$

$$W_{corr} = \frac{RT}{Nh} e^{\frac{\Delta S^*}{R}} e^{\frac{-\Delta H^*}{RT}} \quad (10)$$

where E_a is the activation corrosion energy, P is a constant term, R is the universal gas constant, T the absolute temperature, h is the Planck's constant, N is the Avogadro's number. ΔH^* and ΔS^* the enthalpy and entropy of activation, respectively.

E_a was calculated from the slopes of $\ln W_{corr}$ against $1/T$ provides straight lines as exposed in Fig.10. Moreover, Figure.11 shows the plots of $\ln (W_{corr}/T)$ against $1/T$ of inhibitor at different concentrations of essential oil. Straight lines are acquired with a slope of $(-\Delta H^*/R)$ and an intercept of $\ln(R/(N \times h)) + \Delta H^*/R$ from which the values of ΔH^* and ΔS^* are determinate, respectively.

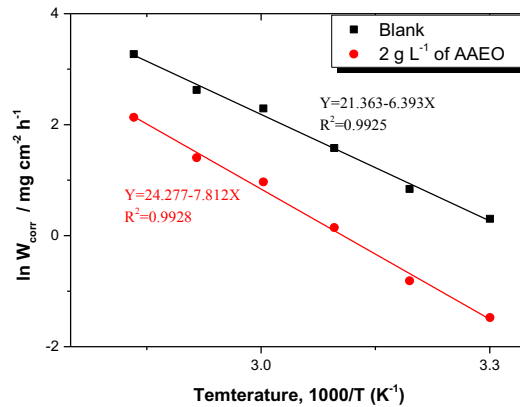


Figure10: Transition state plots of metal in aggressive solution (1 M HCl) in absence and presence 2 g L⁻¹ of AAEO.

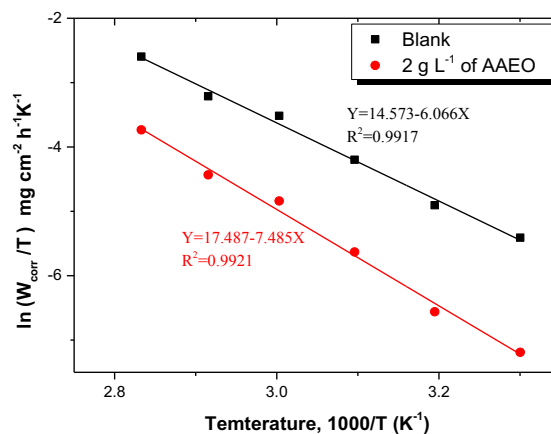


Figure11: modified Arrhenius plots $\ln(W_{corr}/T)$ vs. $1/T$ in 1 M HCl in absence and presence 2 g L⁻¹ of AAEO.

The corresponding results of P , E_a , ΔH^* and ΔS^* are summarized in Table 5.

Table 5: Activation parameters P , E_a , ΔH^* , ΔS^* for mild steel in aggressive solution 1 M HCl with and without 2 g L⁻¹ of AAEO.

	Blank	AAEO
Constant, P / mg cm ⁻² h ⁻¹	1897114719	34964531538
E_a / kJ mol ⁻¹	53.15	64.95

$\Delta H^*/\text{kJ mol}^{-1}$	50.43	62.23
$\Delta S^*/\text{J mol}^{-1}\text{K}^{-1}$	-76.37	-52.15

Figure.10 showed that all the linear regressions coefficient (R^2) is very close to unity. Popova [45] has mentioned that the diminution of the protection efficiency with increasing of temperature, which corresponds to a higher value of E_a , when compared to that in the blank, is considered as an indication of physisorption. From Table 5, we remark that E_a changes slightly with AAEO. The higher value of E_a and P in essential oil presence when compared to that in the blank are explained with the processing of specific interaction between AAEO and the mild steel surface. On the other hand, ΔH^* it is positively reflecting the endothermic reaction of metalcorrosion process [25] and indicated that the dissolution of metal was slow in the presence of AAEO[46]. Consequently, ΔS^* in with and without of essential oil was larger and negative. However, this result suggests that a diminution in disorder takes place, move pass from reactant to the activated complex [22].

3.7. Adsorption isotherm

For obtained additional knowledge concerning the mechanism of adsorption of AAEO on the mild steel, the experimental data have been investigated with various adsorption isotherms[47]. However, the adsorption of AAEO compounds at the mild steel/aggressive solution (1M HCl) interface involves of the substitution of H_2O molecules by essential oil compounds which can be expressed as (Equation 11)[2]:



where $Com_{(sol)}$ is the essential oil compounds containing in the aggressive solution, $Com_{(ads)}$ is AAEO compounds adsorbed on the mild steel surface, and x is the numeral of H_2O molecules displaced by AAEO compounds. The experimental data were fitting to a some of the adsorption isotherms, i.e., Langmuir, El-Awady, Flory-Huggins, Temkin, Freundlich, and Frumkin. It is noted that the surface coverage (θ) values are obtained from gravimetric, potentiodynamic polarization methods (Tafel, Stern & Geary), and EIS measurements at various concentrations of essential oil. according to the following Equation 12:

$$\theta = \frac{\eta\%}{100} \quad (12)$$

Indeed, θ is associated to the essential oil concentration C_{inh} via the Equations [7,48–51]:

Langmuir
$$\frac{C_{inh}}{\theta} = \frac{1}{K_{ads}} + C_{inh} \quad (13)$$

El-Awady
$$\log\left(\frac{\theta}{1-\theta}\right) = y \log K_{ads} + y \log C_{inh} \quad (14)$$

Flory-Huggins
$$\log\left(\frac{\theta}{C_{inh}}\right) = \log K_{ads} + x \log(1-\theta) \quad (15)$$

Temkin
$$\theta = -\frac{1}{2 \times a} \ln K_{ads} - \frac{1}{2 \times a} \ln C_{inh} \quad (16)$$

Freundlich
$$\ln \theta = \ln K_{ads} + z \ln C_{inh} \quad (17)$$

Frumkin
$$\ln C_{inh} \left(\frac{1-\theta}{\theta}\right) = -\ln K_{ads} + 2d\theta \quad (18)$$

where x constitutes a measure of the value of adsorbed H_2O molecules replaced by a given AAEO molecules. $1/y$ gives the number of H_2O molecules removed by 1 compound of essential oil. Z is the parameter describing the nature of mild steel/medium interface, where $0 < Z < 1$. The parameters a and d represent the interactions factors among adsorbed molecules (these interaction parameters may be positive or negative: a or $d < 0$ indicates repulsion force, a or $d > 0$ shows the lateral attraction among adsorbed organic molecules).

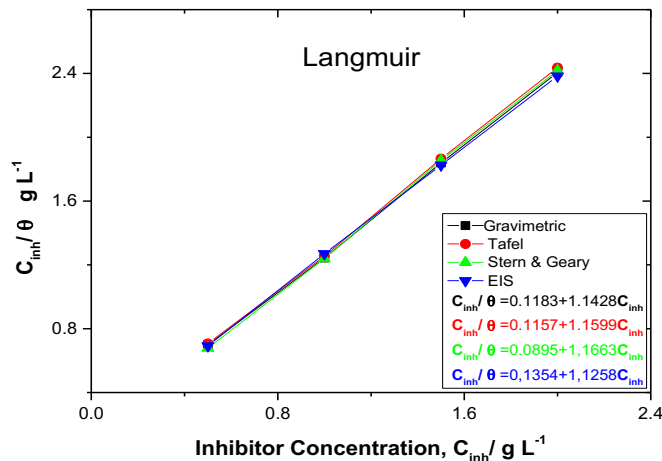


Figure12: Langmuir isotherm model of essential oil onto the mild steel at 303K obtained from four undertaken methods.

The experimental results and the fitting data were observed in Figure.12. To select the isotherm that good fit to experimental results, R^2 was utilized. The best fitting was calculated with the value of R^2 reaches to 0.999 and the fitted line gives a slope very close to one, which suggests that the experimental results can be obtained by Langmuir isotherm [27]. This isotherm postulates that the energy of adsorption is independent of θ and there is no interaction among the adsorbed compounds contained in the essential oil. Moreover, Langmuir isotherm accepts that the mild steel surface contains a fixed number of adsorption sites, and each holds one adsorbed species [17]. It is essential to note that the investigation of the adsorption isotherm compartment, utilizing eco-friendly inhibitors, in terms of the standard Gibbs energy ($\Delta_r G^0_{ads}$) value, is impossible because the compound total of AAEO is unknown. Different researchers [1,9,38,50], in their investigation on acid corrosion with eco-friendly inhibitors, noted similar limitation.

Conclusion

Chemical and electrochemical examination using AAEO as eco-friendly corrosion inhibitor concluded that:

1. The protection efficiency rise with the rising of AAEO concentration reaches to 83.92%, but diminutions with the rise of temperature.
2. SEM examination of the mild steel surface supported well the presence of protective adsorbed film.
3. The adsorbed film blocks the reduction of hydrogen ions and protects the mild steel against corrosion in 1M HCl.
4. Tafel polarization revealed that AAEO acts as a mixed type inhibitor.
5. Nyquist curves for AAEO concentrations contained a capacitive loop at HF followed up by a small inductive loop at LF and the best equivalent circuit was used for fitting the experimental data.
6. The protection efficiency obtained from different measurements such as gravimetric, Tafel, LPR and EIS are in good agreement and in similar trends.
7. The constant term and the apparent activation energy value considerably increased after addition of the essential oil, suggesting that AAEO undergoes physisorption mechanism on the metal surface.

References

1. Raja P.B.; Qureshi A.K.; Abdul Rahim A.; Osman H. & Awang K., *Corros. Sci.*, 69 (2013) 292.
2. Solmaz R., *Corros. Sci.*, 79 (2014) 169.
3. ASTM MNL 20, Corrosion Tests and Standards: Application and Interpretation-Second Edition, (2009) 1–886.
4. Kowsari E.; Arman S.Y.; Shahini M.H.; Zandi H.; Ehsani A.; Naderi R.; Pourghasemi Hanza A. & M. Mehdipour., *Corros. Sci.*, 112 (2016) 73.
5. Salarvand Z.; Amirnasr M.; Talebian M.; Raeissi K. & Meghdadi S., *Corros. Sci.*, 114 (2016) 133.
6. Yildiz R., *Corros. Sci.*, 90 (2015) 544.
7. Sığircık G.; Yildirim D. & Tüken T., *Corros. Sci.*, 120 (2017) 184.

8. Ayers R.&Hackerman N. , *J. Electrochem. Soc*, 110 (1963) 507-513.
9. El Hamdani N.;Fdil R.;Tourabi M.;Jama C. & Bentiss F., *Appl. Surf. Sci*, 357 (2015) 1294.
10. Mourya P.; Banerjee S.& Singh M.M., *Corros. Sci*, 85 (2014) 352.
11. Bentrach H. ;Rahali Y. &Chala A., *Corros. Sci*, 82 (2014) 426.
12. Fiori-Bimbi M. V. ; Alvarez P.E. ;Vaca H.&Gervasi C.A., *Corros. Sci*, 92 (2015) 192.
13. Quraishi M.A. ; Singh A. ; Kumar V. ; Kumar D. & Kumar A., *Mater. Chem. Phys*, 122 (2010) 114.
14. Hussin M.H. ; Abdul A. ; Nasir M. ; Ibrahim M. & Brosse N., *Measurement*, 78 (2016) 90.
15. Boumhara K.;Tabyaoui M.;Jama C.& Bentiss F., *J. Ind. Eng. Chem*, 29 (2015) 146.
16. Zerga B. ; Sfaira M. ; Rais Z. ; Ebn Touhami M. ; Taleb M. ; Hammouti B. ;Imelouane B. &Elbachiri A., *Matériaux Tech*, 97 (2009) 297.
17. Halambek J.;Berković K. &Vorkapić-Furač J., *Corros. Sci*, 52 (2010) 3978.
18. Council of Europe, European Pharmacopoeia, 5th Ed, EDQM, 2005.
19. McCafferty E., *Corros. Sci*, 47 (2005) 3202.
20. Rochdi A.; Kassou O.; Dkhireche N.; Tourir R.; El Bakri M.; Ebn Touhami M.; Sfaira M.; Mernari B. & Hammouti B., *Corros. Sci*, 80 (2014) 442.
21. Tang Y., Zhang F., Hu S., Cao Z., Wu Z.& Jing W., *Corros. Sci*, 74 (2013) 271.
22. Hegazy M.A.; Hasan A.M.;Emara M.M.; Bakr M.F.& Youssef A.H., *Corros. Sci*, 65 (2012) 67.
23. Bouayad K. ;Rodi Y. K. ; El Ghadraoui E. H. ;Elmsellem H. ;Ouzidan Y. ;Elmahdi B. ;Essassi E. M. ; Chetouani A.& Hammouti B., *Moroccan J. Chem*, 2(2017) 285.
24. Negm N.A.;Kandile N.G.;Badr E.A.& Mohammed M.A., *Corros. Sci*, 65 (2012) 94.
25. Bagga M.K.;Gadi R.; Yadav O.S.; Kumar R.; Chopra R.& Singh G., *J. Environ. Chem. Eng*. 4 (2016) 4699.
26. Halambek J.;Berkovic 'K.&Vorkapic '-Furac J., *Corros. Sci*, 52 (2010) 3978.
27. Jeroundi D.;Chakroune S.;Elmsellem H.; El Hadrami E. M.;BenTama A.;Elyoussfi A.;Dafali A.;Douez C.& Hafez B., *J. Mater. Environ. Sci*,9(2018)334.
28. Kicir N. ;Tansu G. ;Erbil M. &Tüken T., *Corros. Sci*, 105 (2016) 88.
29. Behpour M.; Ghoreishi S.M.;Khayatkashani M.&Soltani N., *Corros. Sci*, 53 (2011) 2489.
30. Zarrok H.;Zarrouk A.; Hammouti B.;Salghi R.;Jama C.& Bentiss F., *Corros. Sci*, 64 (2012) 243.
31. Solmaz R., *Corros. Sci*, 81 (2014) 75.
32. Solmaz R., *Corros. Sci*, 52 (2010) 3321.
33. Amin M.A.& Khaled K.F., *Corros. Sci*, 52 (2010) 1762.
34. Benghalia M. A. ; Fares C. ; Khadraoui A.;Meliani M. H.;Obot I. B.;SorrourA.;DmytrakhM. & Azari Z., *Moroccan J. Chem*, 1 (2018)51.
35. Ahamad I.; Prasad R.& Quraishi M.A., *Corros. Sci*, 52 (2010) 933.
36. Rbaa M.; Galai M.; El Faydy M.; Lakhrissi Y.; Ebntouhami M.; Zarrouk A. &Lakhrissi B., *J. Mater. Environ. Sci.*, 9 (2018)172.
37. El Bribr A. ;Tabyaoui M. ;Tabyaoui B. ; El Attari H.& Bentiss F., *Mater. Chem. Phys*, 141 (2013) 240.
38. Banerjee S.; Srivastava V.& Singh M.M., *Corros. Sci*. 59 (2012) 35.
39. Labjar N.;Lebrini M.; Bentiss F.;Chihib N.E.; El Hajjaji S.&Jama C., *Mater. Chem. Phys*. 119 (2010) 330.
40. Khaled K.F.& Amin M.A., *Corros. Sci*, 51 (2009) 1964.
41. Gojic M., *Corros. Sci*, 43 (2001) 919.
42. Bentiss F.;Lebrini M.;Lagrenée M.;Traisnel M.;Elfarouk A.&Vezin H., *Electrochim. Acta*. 52 (2007) 6865.
43. Barsoukov E., Macdonald J.R., Impedance Spectroscopy, 2005.
44. Hassan H.H.; Amin M.A.;Gubbala S.&Sunkara M.K., *Electrochim. Acta*, 52 (2007) 6929.
45. Popova A., *Corros. Sci*, 49 (2007) 2144.
46. Kumar K.P.V.; Pillai M.S.N.&Thusnavis G.R., *J. Mater. Sci. Technol*, 27 (2011) 1143.
47. ChebliH.;Batah A.; Asdadi A.; Zaafrani M.; IdrissiHassani L.; Bounimi S.; Chebli B.; &Salghi R., *Appl. J. Environ. Eng. Sci*, 3 (2017) 131.
48. Nataraja S.E.; Venkatesha T. V.; Manjunatha K.; Poojary B.; Pavithra M.K.&Tandon H.C., *Corros. Sci*. 53 (2011) 2651.
49. Dahiya S.; Lata S.; Kumar R.; Yadav O.S., *J. Mol. Liq*, 221 (2016) 124.
50. Khadraoui A.;Khelifa A.; Hadjmeliani M.; Mehdaoui R.; Hachama K.; Tidu A., Azari Z.; Obot I.B. & Zarrouk A., *J. Mol. Liq*, 216 (2016) 724.
51. El-Awady A.A.; Abd-El-Nabey B.A. & Aziz S.G., *J. Electrochem. Soc*, 139 (1992) 2149.

(2018) ; <http://www.jmaterenvirosci.com>